THE JOURNAL OF BIOLOGICAL CHEMISTRY VOL. 280, NO. 52, pp. 43209–43217, December 30, 2005

Identification of the Preprotein Binding Domain of SecA*[S]

Received for publication, September 12, 2005, and in revised form, October 12, 2005 Published, JBC Papers in Press, October 21, 2005, DOI 10.1074/jbc.M509990200

Efrosyni Papanikou[‡], Spyridoula Karamanou[‡], Catherine Baud[‡], Miriam Frank[‡], Giorgos Sianidis[‡], Dimitra Keramisanou[§], Charalampos G. Kalodimos[§], Andreas Kuhn[¶], and Anastassios Economou[‡1]

From the [‡]Institute of Molecular Biology and Biotechnology, F.O.R.T.H. and Department of Biology, University of Crete, P.O. Box 1527, GR-711 10 Iraklio, Crete, Greece, [§]Chemistry Department, Rutgers University, Newark, New Jersey 07102, and [¶]Institute of Microbiology and Molecular Biology, University of Hohenheim D-70593 Stuttgart, Germany

SecA, the preprotein translocase ATPase, has a helicase DEAD motor. To catalyze protein translocation, SecA possesses two additional flexible domains absent from other helicases. Here we demonstrate that one of these "specificity domains" is a preprotein binding domain (PBD). PBD is essential for viability and protein translocation. PBD mutations do not abrogate the basal enzymatic properties of SecA (nucleotide binding and hydrolysis), nor do they prevent SecA binding to the SecYEG protein conducting channel. However, SecA PBD mutants fail to load preproteins onto SecYEG, and their translocation ATPase activity does not become stimulated by preproteins. Bulb and Stem, the two sterically proximal PBD substructures, are physically separable and have distinct roles. Stem binds signal peptides, whereas the Bulb binds mature preprotein regions as short as 25 amino acids. Binding of signal or mature region peptides or full-length preproteins causes distinct conformational changes to PBD and to the DEAD motor. We propose that (*a*) PBD is a preprotein receptor and a physical bridge connecting bound preproteins to the DEAD motor, and (*b*) preproteins control the ATPase cycle via PBD.

Most bacterial secretory proteins are synthesized with amino-terminal signal peptides and are exported through the Sec pathway. This process is best understood in *Escherichia coli*. The SecA ATPase subunit interacts with most of the components of the reaction, including the SecYEG membrane "channel," chaperones, preprotein signal and mature domains, acidic phospholipids, and nucleotides. Preproteins bind to SecYEG-associated SecA with high affinity, and this interaction initiates cycles of ATP-driven SecA insertion and deinsertion at SecYEG (1–3).

SecA is a Superfamily 2 RNA helicase (4–6) that adapted to translocating polypeptides. It contains the characteristic DEAD/DEXH ATPase core structure (Fig. 1, *A* and *B*; hereafter referred to as the "DEAD motor") with the nine Superfamily 2 motifs (Fig. 1*B*) (4, 6–11). The DEAD motor comprises two domains: the discontinuous nucleotide-binding domain (NBD[2]; aa 1–220 and 378–420; Fig. 1, *A* and *B*, *blue*) and IRA2 (intramolecular regulator of ATPase domain) (aa 421–610; Fig. 1, *A* and *B*, *light blue*) that form between them a mononucleotide crevice (7, 9, 10, 12).

DEAD motors acquire specificity for different catalytic processes through add-on nonhomologous structural appendages (8, 11). SecA has two such structures (12–14) (Fig. 1, *A* and *B*): (*a*) the C-domain (aa 611–832), which is fused C-terminally to the IRA2 domain of the DEAD motor and regulates its mobility and properties by "stapling" together NBD and IRA2 (14, 15), and (*b*) a second appendage (aa 221–377) of unknown function, which forms an independent structural domain (Fig. 1*A*, *magenta*) that comprises a bilobate "Bulb" bridged with NBD through a "Stem" formed of two anti-parallel β strands (β1 and β7; $Stem_{out}$ and $Stem_{in}$, respectively; Fig. 1, *B* and *C*). The Stem is physically "rooted" in NBD (Fig. 1, *A* and *C*) without disturbing its structural integrity. As it protrudes out of NBD, the aa 221–377 appendase "embraces" loosely, mainly through Bulb-mediated contacts, parts of the C-domain (9, 10, 15).[3] At least two distinct Bulb conformational states have been identified in crystallographic studies of *Bacillus subtilis* SecA (10, 16).

Cytoplasmic SecA is stabilized in a quiescent ADP-bound state (7, 14, 15, 17) with suppressed preprotein binding (18) and ATP catalysis (19). Interaction of preproteins with membrane-bound SecA (18, 20) triggers multiple cycles of ATP hydrolysis (19, 21, 22), and this allows processive preprotein translocation (1, 23).

Numerous studies have demonstrated preprotein binding to SecA (12, 19, 24–29). However, where precisely on SecA preproteins bind and how they stimulate its ATPase remains unresolved. This central question must be answered before the molecular basis of SecA-dependent preprotein movement through translocase can be understood. The Stem and Bulb substructures have been indirectly implicated in preprotein binding (12, 24). Isolated NBD fragments that also include the β1 strand (Fig. 1*C*) retain signal peptide binding of high affinity, whereas deletion of the β1 strand in SecA prevents signal peptide binding (12). However, this study could not conclusively determine whether signal peptide binding occurs on the Stem or whether the Stem is indirectly involved in binding. In another study, N-terminal SecA fragments that were refolded from inclusion bodies and included parts of the Bulb (aa 267–340) were cross-linked to a complete preprotein (24). However, the specificity of this reaction is unclear, since (*a*) cross-linking occurred only when SecA was partially "reconstituted" by mixing N-terminal fragments together with C-terminal peptides, and (*b*) the cross-linker used was nonspecific.

Now we have investigated the functional role of the SecA domain that encompasses residues 221–377. We demonstrate that this domain is essential for cell viability, protein translocation, and preprotein-stimulated translocation ATPase. Moreover, we provide direct evidence that this region is essential for preprotein loading onto SecYEG-containing membranes and retains the ability to bind preproteins in solution even

* This work was supported by European Union Grants RTN1-1999-00149 QLRT-2000-00122, and QLK3-CT-2000-00082, Pfizer, Inc., and Greek General Secretariat of Research Grants 01AKMON46, PENED2001, and PENED03ED623. The costs of publication of this article were defrayed in part by the payment of page charges. This article must therefore be hereby marked "*advertisement*" in accordance with 18 U.S.C. Section 1734 solely to indicate this fact.

[S] The on-line version of this article (available at http://www.jbc.org) contains supplemental Figs. 1–4.

[1] To whom correspondence should be addressed: Institute of Molecular Biology and Biotechnology, F.O.R.T.H. and Dept. of Biology, University of Crete, P.O. Box 1527, GR-711 10, Iraklio, Crete, Greece. Fax/Tel.: 30-2810-391166; E-mail: aeconomo@imbb.forth.gr.

[2] The abbreviations used are: NBD, nucleotide binding domain; PBD, preprotein binding domain; IMV, inner membrane vesicle; MANT-ADP, 2′ (or 3′)-*O*-(*N*- methylanthraniloyl) adenosine 5′-diphosphate; aa, amino acid(s).

[3] Y. Papanikolau, M. Papadovassilaki, R. B. G. Ravelli, A. McCarthy, S. Cusack, A. Economou, and K. Petratos, manuscript in preparation.

when detached from SecA. This region is therefore a preprotein-binding domain (PBD). Further, we show that PBD has two distinct domains with distinct subsites (Stem and Bulb) with discrete functional subsites. SecA binds signal peptide through the PBD Stem and mature regions through the PBD Bulb. These binding events influence PBD and DEAD motor conformation and subsequently DEAD motor ATP hydrolysis. We propose that PBD due to its strategic location acts as a physical and functional bridge between preproteins and the ATPase DEAD motor.

EXPERIMENTAL PROCEDURES

Bacterial Strains and Recombinant DNA Experiments—E. coli strains were grown and manipulated as described (7, 14, 30).

To construct *his_{10}-secAΔBulb(Δ233–365)*, we first constructed *secA(N1–232)* by PCR using as template pIMBB10(*secA*) (14), forward primer X157 (5′-GGCCCGTACATATGCTAATCAAATTGTTAAC-3′; introduced cloning sites are underlined), and reverse primer X176 (5′-CCGGACCTCGAGGCTGTCTTCTGCCGGGCC-3′). The 0.7-kb PCR fragment was digested with NdeI/XhoI and ligated to the same sites of pET16b (Invitrogen), resulting in pIMBB264. Then, *secAN366–901* was constructed by PCR using as template pIMBB10, forward primer X177 (5′-CCGGACCTCGAGGGCGCAGGCCA-GAACGAAAACCAAACGCTG-3′), and reverse primer X131 (5′-CG-GCAGGGATCCTTATTGCAGGCGGCCATGGC-3′). The 1.6-kb PCR fragment was digested with XhoI/BamHI and ligated to the same sites of pET16b resulting in pIMBB274. Finally, pIMBB275 (*his_{10}-secAΔBulb*) derived from cloning the 0.8-kb XbaI/XhoI restriction fragment of pIMBB264 into the corresponding sites of pIMBB274. pIMBB277 (*his_{10}-N68ΔBulb*) was generated by cloning the 0.5-kb KpnI/SnabI restriction fragment of pIMBB8 into the corresponding sites of pIMBB275.

his_{10}-SecA(W349A) was constructed by PCR using as template pIMBB7 (14), forward primer X182 (GGCCCGCAGTACGTTC), reverse primer X198 (CCGTCGCGCGTCCGATGG), and mutagenesis primer X196 (CTGATCGATGAAGCGCGTAC). The 0.5-kb PCR fragment was digested with BclI/BglII and cloned in the corresponding sites of pIMBB7, resulting in pIMBB389.

his_{10}-secAΔ219–240 was constructed as described (12, 13). *his_{10}-secAΔ351–368* was constructed by subcloning the 2.5-kb NcoI fragment from pGJ5 (13) to the corresponding site of pIMBB7, resulting in pIMBB83.

proM13CH5EE-his_6 is a mutant derivative of the major coat protein of phage M13 that contains an insertion of two Glu residues (underlined) and a mutation (S21F; boldface type) that prevents signal peptidase cleavage (complete sequence: MKKSLVLKAS VAVATLVPML FFAAEEEGDDPA KAAFNSLQAS ATEYIGYAWA MVVVIVGATI GIKLFKKFTS) (31). CH5EE-His_6, the mature domain of a mutant derivative, was constructed in two steps as described (32). The *CH5EE(W49F)-his_6* derivative was constructed by oligonucleotide-directed mutagenesis (33). CH5EE24–48 (complete sequence: AEEEGDDPA KAAFNSLQAS ATEYIGC) was prepared by chemical synthesis (Alta Bioscience).

his_{10}N219–379 was constructed by PCR using pIMBB7 (*his_6secA*) (7) as template, forward primer X241 (5′-GGGAATTCCATATGGCGCGTACACCGCTGATCATTTCC-3′), and reverse primer X242 (5′-GCGGGATCCTTAGTTCTGGAAGGTGATCGAAGCCAG-3′). The NdeI/BamHI fragment from the PCR was inserted into pET16b, resulting in pIMBB469.

Membrane Flotation Experiments—Ultracentrifugal sedimentation experiments were carried out in a bench-top ultracentrifuge (TLX120 Optima; TLA120.2 rotor; Beckman), using polypropylene tubes (0.2 ml) as described (34, 35). Reactions (15 μl in buffer B (50 mM Tris-Cl, pH 8, 50 mM KCl, 5 mM $MgCl_2$)) containing SecA or SecAΔBulb (0.5 μg) in the presence or absence of inner membrane vesicles (IMVs) (≤3 μg) and proOmpA-His (0.12 μg) (36) were adjusted to 1.74 M final sucrose concentration and deposited at the bottom of the tube. Samples were overlaid with one layer (20 μl) of 1.6 M sucrose and two consecutive layers (75 μl) of 1.4 and 1.25 M sucrose in buffer B following centrifugation (4 °C; 436,000 × *g*; 180 min). Nine fractions of 25 μl were removed, analyzed by SDS-PAGE, and visualized by immunostaining. SecA was visualized with α-SecA antibodies. proOmpA was immunostained with α-hexahistidinyl antibodies to selectively label freshly bound proOmpA and not the abundant indigenous OmpA population in the IMVs. Flotation of IMVs inside the gradient was monitored by immunodetection of the integral membrane protein SecY.

NMR Spectroscopy—Isotopically labeled samples for NMR studies were prepared by growing the cells in M9 media. All NMR spectra were recorded on a Varian 600-MHz spectrometer. Sequential assignment of the ^{1}H, ^{13}C, and ^{15}N protein chemical shifts of N219–379 was achieved by means of through-bond heteronuclear scalar correlations along the backbone using conventional three-dimensional pulse sequences (37).

Miscellaneous—Biochemical assays and spectroscopies were as described (1, 7, 12, 14, 18). Fluorescence measurements were carried out with a Cary Eclipse fluorimeter (Varian) as described (15). Radioactivity was quantitated by phosphorimaging (Storm 840; Amersham Biosciences). Binding and kinetic data were analyzed using Prism (GraphPad) or Origin (Microcal), and structures were visualized with SwissPDBViewer.

Chemicals and Biochemicals—Proteases, inhibitors, and nucleotides were from Roche Biosciences; all other chemicals were from Sigma. DNA enzymes were from Minotech; oligonucleotides were from MWG; dNTPs were from Promega. [γ-^{32}P]ATP (5000 Ci/mmol), [^{35}S]methionine (1000 Ci/mmol), and chromatography materials (except Ni^{2+} affinity; Qiagen) were from Amersham Biosciences. Biochemicals were purified as described (7, 14, 19, 36, 38).

RESULTS

PBD Is Essential for SecA-dependent Translocation—To analyze the effect of PBD on SecA function, we used the following mutants of oligohistidinyl-tagged SecA (Fig. 1*C*): SecAΔ219–240, which lacks the $Stem_{out}$ (12, 13); SecAΔ351–368, in which a 17-amino acid deletion removes the highly conserved helix 4 of Bulb 2 (13); SecAΔ233–365 (hereafter SecAΔBulb), which is missing the entire Bulb region but retains β1 and β7 of the Stem joined directly with a linker; and SecA(W349A), in which a highly conserved aromatic residue found in all SecA proteins is substituted by alanine.

The ability of SecA PBD mutants carried on a plasmid to rescue the BL21.19 *secAts* strain (30) at 42 °C was examined (Fig. 1*D*). None of the deletion mutants could complement BL21.19 *in vivo*, whereas *secA(W349A)* could, albeit poorly.

Purified SecA PBD mutant proteins are chromatographically stable, dimeric (supplemental Fig. 1) proteins and were tested for their ability to support ATP-dependent translocation of the model preprotein [^{35}S]proOmpA into SecYEG-proteoliposomes (Fig. 1*E*). In agreement with the *in vivo* complementation test (Fig. 1*D*), SecA(W349A) (Fig. 1*E*, *lane 8*) retains some translocation activity compared with SecA (*lane 3*), whereas no translocation was detected with the deletion mutants (*lanes 5–7*).

It became clear from the above results that PBD is essential for SecA-mediated protein translocation. To understand at which step of the

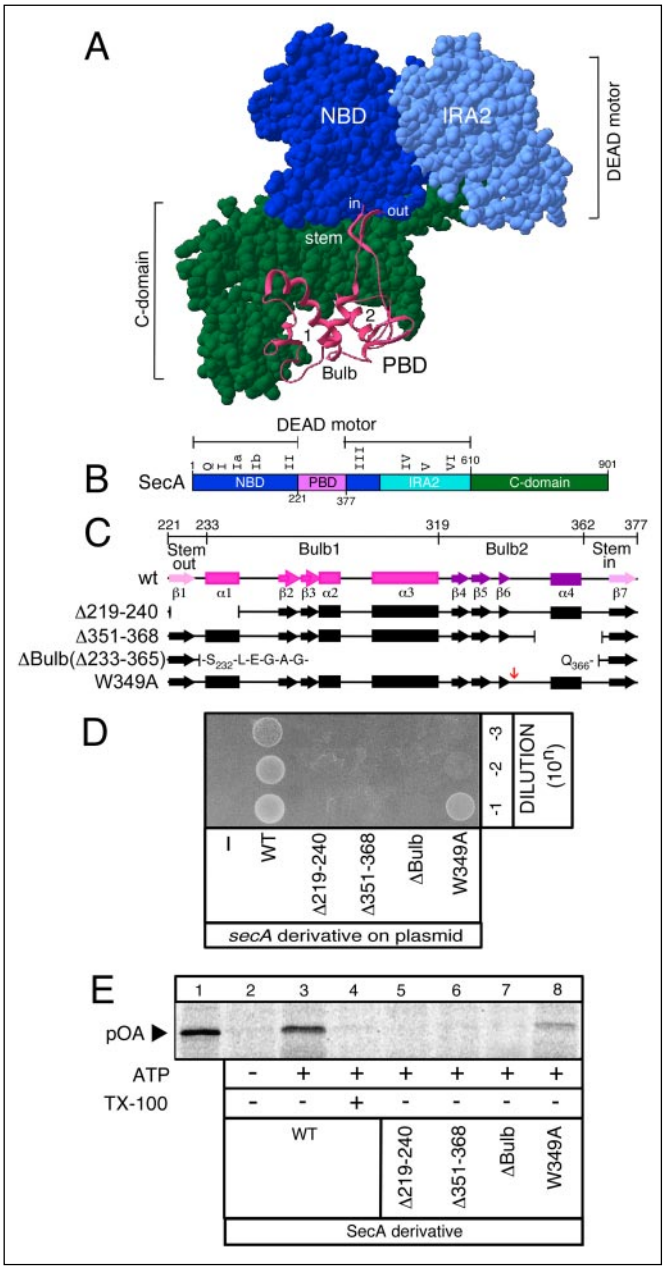

FIGURE 1. **SecA PBD domain and mutants.** *A*, space-filling model of *B. subtilis* SecA (pdb code 1M6N) (10) with PBD in a *ribbon representation*. *B*, linear schematic of the SecA protein. *Latin numerals*, helicase Superfamily 2 motifs. *C*, map of the SecA PBD region. Deletion and point mutants and secondary structure elements of PBD are indicated. *Red arrow*, site of W349A mutation. *D*, *in vivo* complementation test of the BL21.19 *secAts* strain (30) using *secA* PBD mutants. BL21.19 cultures carrying pET5 vector alone or its derivative with cloned *secA*, *secA*Δ219–240, *secA*Δ351–368, *secA*ΔBulb, or *SecA(W349A)* genes grown at 30 °C were adjusted to the same density. The indicated dilutions (10^{n}) were spotted on LB/ampicillin plates and incubated (20 h; 42 °C). *E*, PBD is essential for SecA-mediated translocation. *In vitro* translocation of [^{35}S]proOmpA into SecYEG-proteoliposomes by the SecA PBD mutants. Assays were performed in 50 μl of buffer B containing the indicated SecA proteins (40 μg/ml), SecB (20 μg/ml), bovine serum albumin (400 μg/ml), [^{35}S]proOmpA (20,000 cpm), and SecYEG-proteoliposomes (250 μg/ml). Reactions were initiated by the addition of 2 mM ATP and incubated for 20 min at 37 °C. After proteinase K treatment (1 mg/ml, 15 min, 4 °C), proteins were precipitated (12.5% (w/v) trichloroacetic acid) and separated on 15% SDS-PAGE. [^{35}S]proOmpA protected from proteinase K treatment was detected by phosphorimaging.

translocation pathway the role of PBD is essential, we proceeded to characterize the effect of the mutations on each step of the reaction.

SecA PBD Mutants Retain Nucleotide Binding and ATP Hydrolysis—To examine the effect of PBD on the ability of SecA to bind nucleotide, we determined the equilibrium binding constants of SecA mutants for nucleotide (TABLE ONE), using a MANT-ADP fluorescence-based assay (15, 21). All mutant proteins retain the ability to bind nucleotide, with either similar (SecAΔ351–368 and SecA(W349A)) or somewhat reduced (SecAΔ219–240 and SecAΔBulb) affinities to that of SecA (TABLE ONE).

TABLE ONE

Equilibrium dissociation constants of SecA derivatives for MANT-ADP determined at 4 °C, as described (6)

Protein	K_D
	μM
SecA	0.14 ± 0.02
SecAΔ219–240	1.6 ± 0.4
SecAΔ351–368	0.35 ± 0.13
SecAΔBulb	2.7 ± 0.4
SecA(W349A)	0.14 ± 0.05

Binding of ADP by SecA causes conformational changes that lead to its thermal stabilization (7, 10, 14, 39). To examine whether ADP binding elicits a similar conformational change in SecA PBD mutants, we monitored intrinsic Trp fluorescence upon thermal melting of the mutant proteins in the presence or absence of ADP (15, 21). Under these experimental conditions, the $T_{m(app)}$ of SecA increases upon ADP binding by 5 °C (TABLE TWO). All mutants display ADP-driven thermal stabilization, albeit to a different extent than SecA (TABLE TWO).

Finally, to examine the effect of PBD mutations on the ability of SecA to hydrolyze ATP, we determined the K_{cat} for the basal ATPase activity of all SecA PBD mutants. The basal catalytic properties of SecA remained unaffected by mutations in PBD (TABLE THREE).

Mutations within PBD (including complete Bulb removal) abrogated neither basal ATP catalysis nor ADP association to SecA. Therefore, it seemed unlikely that PBD, which is located outside the ATP cleft (Fig. 1*A*), is a physical determinant essential for nucleotide binding to/hydrolysis by the DEAD motor. Instead, PBD could have a regulatory role in DEAD motor catalysis.

SecA PBD Mutants Bind to SecYEG-containing Membranes—To examine the effect of PBD mutations on the ability of SecA to bind to SecYEG and to form the translocase ternary complex, we employed membrane flotation (34, 35). Inverted IMVs, treated with urea to remove endogenous SecA (19), were loaded at the bottom of a sucrose gradient (corresponding to *lanes 7–9* in Fig. 2) and were floated up during ultracentrifugation. Gradient fractions were subsequently analyzed by SDS-PAGE, and the migration position of IMVs in the gradient (Fig. 2*A*, fractions 4 and 5) was identified on Western blots by immunostaining for SecY, the integral membrane subunit of translocase. SecA immunostaining revealed that the IMV preparation used in these experiments was not contaminated by endogenous SecA traces (Fig. 2*B*). SecA alone (Fig. 2*C*) or mixed with IMVs (Fig. 2*D*) were loaded at the bottom of identical sucrose gradients. The position of SecA within the gradient was identified on Western blots by immunostaining with α-SecA antiserum. In the presence of IMVs, a significant portion (>50%) of SecA migrated to the less dense parts of the gradient and was present in the same fractions as the SecYEG-containing IMVs (Fig. 2, compare *D* with *A*). This indicated that SecA was bound to the membrane vesicles. This SecA-SecYEG association (Fig. 2*D*) is independent of nucleotide addition or temperature (data not shown) (3, 18). In contrast, SecA remained at the bottom of the gradient (Fig. 2*C*, *lanes 7* and *8*). All SecA PBD mutants exhibited behavior identical to that of wild type SecA in this assay; they all associated stably with SecYEG-IMVs independently of nucleotide addition or temperature. Here only SecAΔBulb is shown as an example (Fig. 2, compare *E* with *D*).

TABLE TWO

Endothermic transitions of SecA derivatives

The intrinsic tryptophan fluorescence of the proteins was monitored as a function of temperature, as described (6). The $T_{m(app)}$ values of SecA PBD mutants, in the presence or absence of ADP, are shown.

Protein	$T_{m(app)}$		$\Delta T_{m(app)}$
	Without ADP	With ADP	
SecA	42.7	47.8	5.1
SecAΔ219–240	40	41.5	1.5
SecAΔ351–368	41	43.3	2.3
SecAΔBulb	40	43.7	3.7
SecA(W349A)	40	45.9	5.9

TABLE THREE

Steady state basal ATPase kinetic constants of SecA PBD mutants, as described (6, 7)

Protein	K_{cat}
SecA	4.7 ± 0.4
SecAΔ219–240	5 ± 0.6
SecAΔ351–368	4.5 ± 0.6
SecAΔBulb	5.7 ± 0.7
SecA(W349A)	4.8 ± 0.5

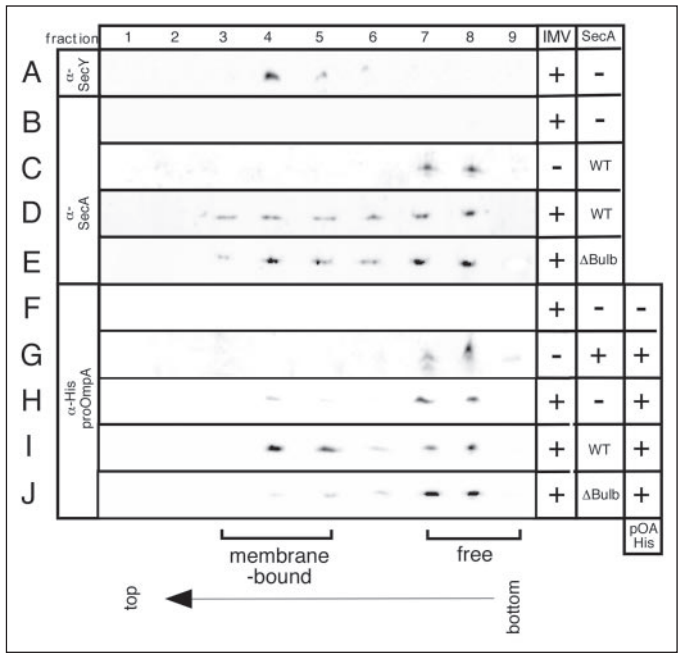

FIGURE 2. **Membrane flotation analysis of SecA derivatives and proOmpA.** *A–E*, recruitment of SecA and SecAΔBulb to SecYEG membranes. Binding of SecA to inverted IMVs studied by flotation analysis using ultracentrifugal isopycnic sedimentation. SecA (0.5 μg) was mixed with IMVs (3 μg of membrane protein) in Buffer B or with the corresponding volume of buffer alone. Following incubation (4 °C for 5 min), reactions (15 μl) were adjusted to a final sucrose concentration of 1.74 M by the addition of 40 μl of 2.4 M sucrose in Buffer B and deposited at the bottom of the centrifugation tube. Samples were overlaid with one layer of 20 μl of 1.6 M sucrose solution and two consecutive layers (75 μl) of 1.4 and 1.25 M sucrose solutions. Following centrifugation (180 min at 436,000 × *g*), fractions (9 × 25 μl) were carefully removed from the meniscus, analyzed by SDS-PAGE, and visualized by immunostaining with an α-SecY (*A*) or an α-SecA (*B–E*) antibody as described (14). *F–J*, analysis of proOmpA recruitment to SecYEG membranes by SecA and SecAΔBulb (as in *B–E*). proOmpA-His (0.12 μg) and SecB (1.2 μg) were added to 15-μl reactions including SecA or SecAΔBulb and IMVs. proOmpA-His was detected by immunostaining with α-hexahistidinyl antibody.

Quantitation of binding affinities by Scatchard analysis confirmed that all SecA PBD mutants retain binding to SecYEG with high affinity (SecAΔBulb K_D = 160 nM; SecA(W349A) K_D = 110 nM, SecAΔ219–240 K_D = 90 nM; SecAΔ351–358 K_D = 100 nM) that is somewhat reduced compared with that of SecA (K_D = 40 nM).

These experiments demonstrated that mutations or deletions within PBD do not prevent SecA binding to SecYEG. Thus, it seems unlikely that PBD is an essential physical determinant for assembly of the SecA-SecYEG holoenzyme.

SecA PBD Mutation Prevents Recruitment of proOmpA to the Translocase—To examine whether mutations in PBD affect SecA interaction with preproteins, we used flotation gradients (Fig. 2, *F–J*). Untreated IMVs alone (Fig. 2*F*) or IMVs mixed with proOmpA complexed with its cognate chaperone SecB (Fig. 2*H*) or mixed with SecA, proOmpA, and SecB (Fig. 2*I*) were fractionated as in Fig. 2, *A–E*. As a control, a mixture of SecA, proOmpA, and SecB was fractionated in the absence of IMVs (Fig. 2*G*). Gradient fractions were analyzed by SDS-PAGE, and the migration position of proOmpA was identified using an α-hexahistidinyl antiserum. This antiserum does not cross-react non-specifically with the IMVs in the gradient (Fig. 2*F*). In the presence of SecA, proOmpA co-migrates in the gradient with SecYEG-containing IMVs (Fig. 2*I*, *lanes 4* and *5*; compare with Fig. 2*A*, *lanes 4* and *5*). In the absence of either SecA (Fig. 2*H*) or of SecYEG-containing IMVs (Fig. 2*G*), proOmpA remained at the bottom of the gradient (Fig. 2, *lanes 7* and *8*). This SecA-dependent proOmpA binding to SecYEG-IMVs was independent of nucleotide or temperature (data not shown). In contrast to SecA, SecAΔBulb failed to recruit proOmpA to the translocase under identical experimental conditions (Fig. 2*J*). Very low amounts of proOmpA, comparable with the background nonspecific binding of proOmpA to IMVs (Fig. 2*H*) (18), are seen to co-migrate with the IMVs.

We conclude that the PBD domain of SecA is essential for preprotein recruitment to the membrane-embedded SecYEG-SecA translocase holoenzyme.

PBD Mutations Compromise Preprotein-stimulated Translocation ATPase—To further study the role of PBD in the SecA-preprotein interaction, we monitored changes in the ATPase activity of SecA (19). Soluble SecA ATPase activity is low ("basal ATPase"; Fig. 3*A*, *lane 1*) (19) and becomes marginally stimulated upon SecA binding to SecYEG at the membrane ("membrane ATPase"; *lane 2*). SecA ATPase becomes significantly stimulated (3–6-fold over membrane ATPase) only following preprotein addition ("translocation ATPase"; Fig. 3, *A* (*lane 3*) and *B*). It was anticipated that mutants that fail to interact with the preprotein will fail to acquire translocation ATPase activity. Indeed, only SecA(W349A) retained some translocation ATPase activity albeit to ~50% of the wild type levels (compare *lane 15* with *lane 3*). No detectable preprotein-stimulated ATPase activity was observed with the SecA PBD deletion mutants (compare *lanes 6*, *9*, and *12* with *lane 3*). Titration of proOmpA demonstrated that the membrane ATPase of SecA PBD mutants could not be stimulated by preprotein even at elevated concentrations (Fig. 3*B*).

These data indicated that SecA PBD mutants fail to acquire preprotein-simulated ATPase activity, suggesting that their interaction with preproteins is compromised.

A Model Preprotein with Stable Binding to Soluble SecA—Collectively, our data suggested that PBD is required for preprotein interaction with SecA (Figs. 2 and 3). We next sought to test whether this reflected direct binding of preproteins to PBD. However, widely used and well characterized model SecA-dependent preproteins, such as proOmpA, are not appropriate for such binding studies, since they bind very poorly to soluble SecA (19, 40).[4] To overcome this limitation, we resorted to using an alternative model preprotein: proM13coatH5EE (hereafter

[4] S. Karamanou and A. Economou, unpublished results.

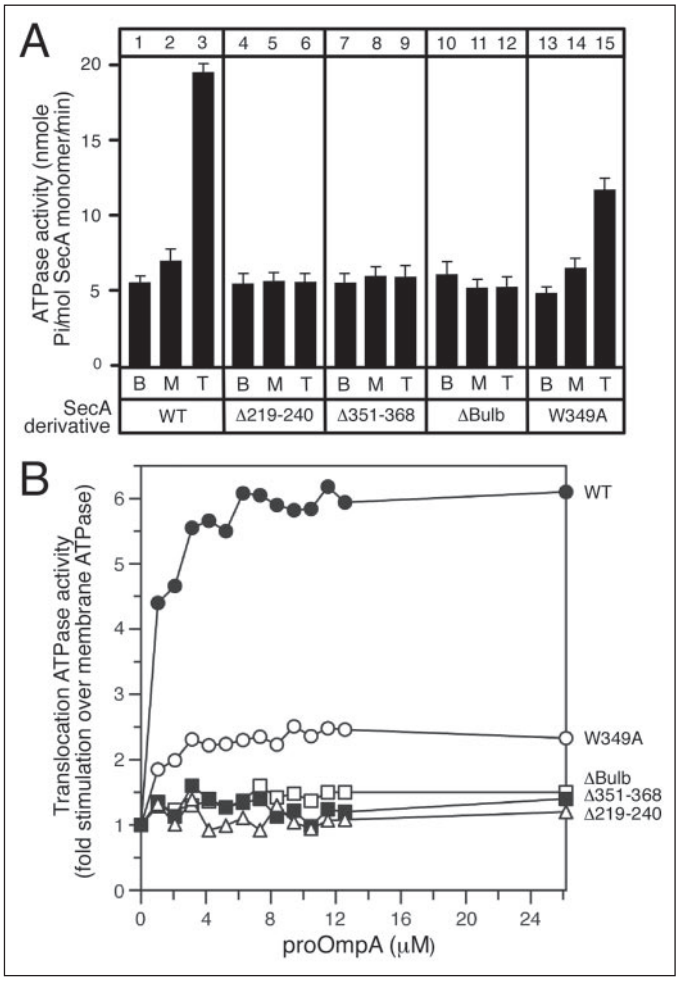

FIGURE 3. **ATPase activities of SecA PBD mutants.** *A*, basal, membrane, and translocation ATPase activities of SecA PBD mutants. The indicated SecA proteins (20 μg/ml) alone (*B*, basal ATPase), mixed with SecYEG-proteoliposomes (200 μg/ml; *M*, membrane ATPase), or mixed with SecYEG-proteoliposomes (200 μg/ml) and proOmpA (30 μg/ml; *T*, translocation ATPase) were incubated (1 mM ATP, 30 min; 37 °C). ATP hydrolysis was measured as described (19). *B*, translocation ATPase activity of SecA PBD mutants (as in *A*) as a function of proOmpA concentration (as indicated). Activity is expressed as *n*-fold stimulation over "membrane ATPase" measured in the absence of proOmpA.

TABLE FOUR

Dissociation constants of SecA, N68, and N219–379 for the preprotein substrates used in this study determined from SPR data ($n = 6$)

Protein	K_D (μM)	
	pCH5EE	CH5EE
SecA	1.96 ± 0.6	3.15 ± 1
N68 (aa 1–610)	3 ± 1.3	2.65 ± 0.9
N1–419	2.6 ± 1	ND[a]
N219–379	24.9 ± 9	ND
N420–610	NM[b]	ND

[a] ND, not determined.
[b] Not measurable.

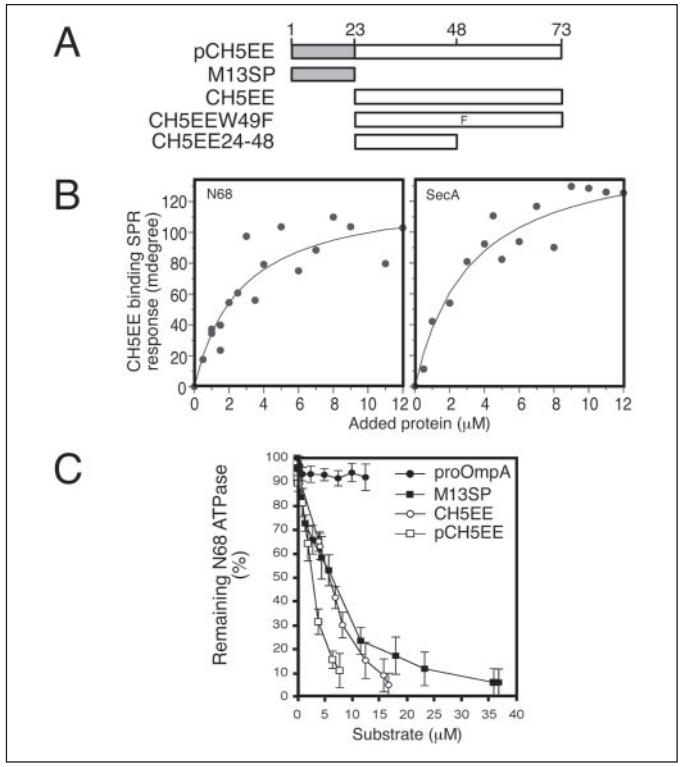

FIGURE 4. **Preprotein binding to SecA and N68.** *A*, map of the model preprotein pCH5EE and derivative constructs. *B*, binding kinetics of N68 and SecA (at the indicated concentrations; Buffer H) to CH5EE immobilized on a surface plasmon resonance biosensor chip. Refractive index changes at equilibrium were plotted against protein concentration (*filled circles*) and are shown together with the fit (*line*) following nonlinear regression analysis. *C*, ATPase suppression assay. N68 (0.3 μM; Buffer B; 1 mM ATP) was supplemented with increasing amounts of the indicated peptides. Basal ATPase (30 min; 37 °C) (19) is expressed as a percentage of the N68 activity in the absence of peptides.

referred to as pCH5EE) (31, 32). pCH5EE, like proOmpA (Fig. 2), requires SecA for its membrane binding (supplemental Fig. 2) and for translocation into the membrane (31) and outcompetes the binding of proOmpA to membranes (31). Its short length, which satisfies a minimal size required for SecA-mediated secretion (73 aa) (41), and its tight binding to soluble SecA (see below; TABLE FOUR) made pCH5EE optimally suited for mapping preprotein binding surface(s) on SecA.

In addition to pCH5EE, the mature region devoid of signal peptide (hereafter referred to as CH5EE) or its derivative CH5EEW49F (Fig. 4*A*) were oligohistidinyl-tagged, overexpressed, and purified (31, 32). The signal peptide of pCH5EE (hereafter M13SP) was chemically synthesized.

Mature Regions of Preproteins Bind to N68—Signal peptides bind to the N68 (a polypeptide that encompasses residues 1–610 of SecA and comprises the NBD, IRA2, and PBD domains) (12, 28). In contrast, direct physical binding of mature preprotein regions to N68 has never been demonstrated. To determine whether mature preprotein regions can bind to N68, CH5EE was immobilized on an optical biosensor, and the equilibrium dissociation constants for SecA as well as for N68 were determined (TABLE FOUR and Fig. 4*B*). Both proteins bind to CH5EE with comparable low micromolar affinities. Similar results were obtained using a CH5EE(W49F) biosensor (data not shown).

To corroborate these findings, we used an activity-based binding assay. Binding of the model signal peptide 3K7L suppresses N68 ATPase (12). As anticipated, M13SP had a similar effect in this functional assay (Fig. 4*C*). The addition of pCH5EE or CH5EE also led to suppression, whereas that of proOmpA did not. This lack of suppression by proOmpA may correlate with its low affinity for soluble SecA (19, 40).

These data demonstrated that the three amino-terminal domains of SecA (610 residues) are necessary and sufficient to bind signal peptide (12) and mature preprotein regions of pCH5EE.

Isolated PBD Binds Preproteins—We next sought to identify which SecA domain present in N68 is responsible for preprotein binding. To this end, we used N1–419, a fragment that contains both the NBD and

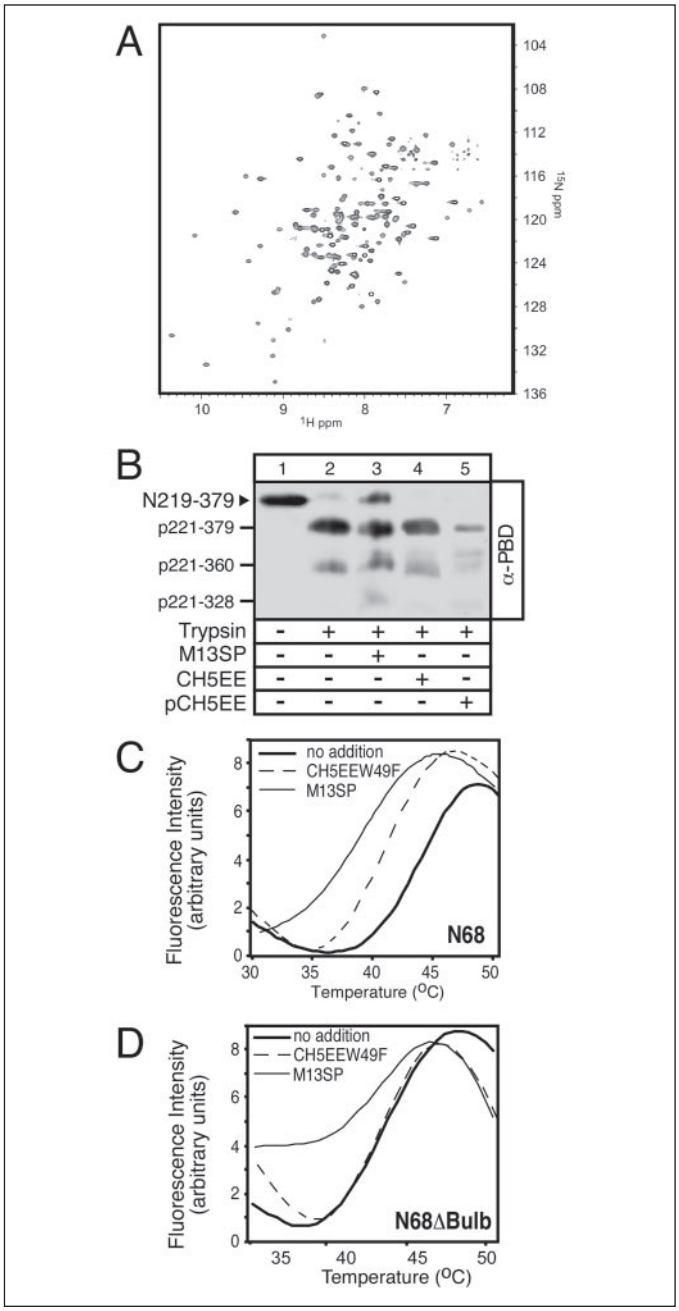

FIGURE 5. **Binding of preprotein segments to PBD.** *A*, two-dimensional ^{1}H-^{15}N heteronuclear single quantum coherence spectrum of N219–379 recorded at 22 °C. The protein (final concentration of 0.5 mM) was dissolved in 50 mM KP_i buffer (pH = 7.0) containing 50 mM KCl and 1 g/liter NaN_3. *B*, limited trypsinolysis of N219–379. N219–379 (9.5 μM) was treated with trypsin (16 μg/ml; Buffer B; 2.5 min; 4 °C) in the absence or presence of the indicated peptides (9.5 μM). Trypsin was inactivated by pefabloc (9 mM). Polypeptides were separated by SDS-PAGE and immunostained by α-PBD domain-specific antibodies (12, 15, 21). Tryptic peptide identity was determined by N-terminal sequencing. A representative of nine experiments is shown. C and D, changes in the intrinsic fluorescence of N68 (*C*) or N68ΔBulb (*D*), (both at 0.73 μM; Buffer B) were monitored at 345 nm as a function of temperature in the absence or presence of the indicated peptides (3.65–5 μM). $n = 6$.

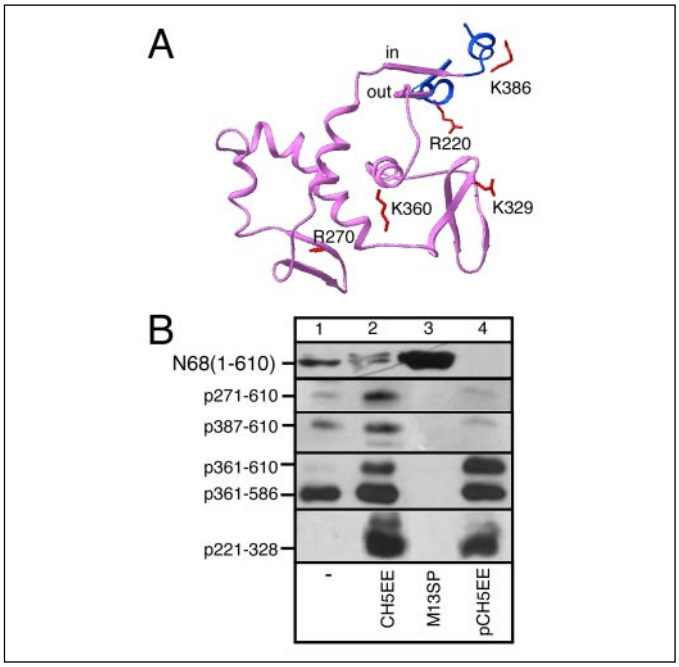

FIGURE 6. **Conformational analysis of DEAD motor-attached PBD in the presence of preprotein moieties.** *A*, *E. coli* PBD tryptic sites are shown on the *B. subtilis* PBD structure (*magenta*). Corresponding residue numbers between the two proteins are as follows (*E. coli*/*B. subtilis*): Arg^{220}/Arg^{218}; Arg^{270}/Lys^{257}; Lys^{329}/Glu^{309}; Lys^{360}/Lys^{340}; Lys^{386}/Arg^{366}. Short adjoining NBD segments (*blue*) are also shown. *B*, limited trypsinolysis of N68 in the absence or presence of the indicated preprotein peptides (29 μM; as in Fig. 5*B*). Following SDS-PAGE, polypeptides were immunostained with α-N68-specific antibodies (12, 15, 21), and their identity was determined by N-terminal sequencing. A representative of six experiments is shown. Identical results were observed when SecA was used in the same assay (data not shown).

PBD domains and N420–610, a fragment that encompasses all of IRA2 (12). In addition, the sequence encoding residues 219–379, that fully encompasses PBD (aa 221–377), was cloned as an independent gene. The derived oligohistidinyl-tagged polypeptide (N219–379) was soluble, chromatographically stable, and monomeric (supplemental Figs. 3 and 4). To determine its folding, N219–379 was isotopically labeled, and its fingerprint two-dimensional ^{1}H-^{15}N heteronuclear single quantum coherence spectrum was recorded by NMR (Fig. 5*A*). Backbone assignment revealed that the Bulb region of N219–379 is well folded in solution, as evidenced by the dispersion of the corresponding peaks. However, the Stem element is clearly unfolded and very flexible even at temperatures as low as 10 °C. Most likely, tethering of the Stem to NBD in SecA is important to stabilize the Stem.

To analyze binding of N1–419, N420–610, and N219–379 to preproteins, we used an optical biosensor with immobilized pCH5EE. The isolated PBD fragment retains binding to immobilized pCH5EE (TABLE FOUR), albeit with reduced affinity compared with SecA and N68. N1–419 binds to pCH5EE with an affinity indistinguishable from that of SecA and N68 (TABLE FOUR). In contrast, no detectable binding was measured with N420–610, indicating that IRA2 is not involved in preprotein binding. We next sought to test the specific role of NBD in the binding reaction constructing and using N1–419ΔBulb in the biosensor system. However, all ΔBulb derivatives tested aggregated on the sensor surface and could not be studied in this assay system (data not shown).

We concluded that isolated PBD can bind preproteins, although optimal binding activity may require either its tethering to NBD or the presence of specific NBD residues.

Isolated PBD Binds both Signal Peptide and Mature Regions—Can N219–379 bind to distinct preprotein moieties? To address this question, we monitored changes in the tryptic accessibility of specific Arg/Lys residues (Fig. 6*A*) upon the addition of either M13SP or CH5EE or pCH5EE (Fig. 5*B*). In the absence of any ligand, trypsin-cleaved N219–379 at Arg^{220} (at the base of the Stem) and at Lys^{360} (located at the Bulb; *lane 2*). The presence of each of the preprotein segments resulted in distinct and characteristic tryptic patterns. In the presence of M13SP, Arg^{220} and Lys^{360} became less accessible (compare amounts of N219–

379 in *lanes 3* and *2*), whereas Lys^{329} became exposed (*lane 3*; see p221–328). The addition of CH5EE (*lane 4*) prevented efficient cleavage at Arg^{360} (compare p221–360 in *lanes 4* and *2*). Finally, the addition of pCH5EE exposed Lys^{329} (compare p221–328 in *lanes 5* and *2*). Under identical conditions, no changes to the tryptic profile of the IRA2 subdomain fragment (Fig. 1*A*) were observed (data not shown).

We concluded from the tryptic accessibility assays that the isolated PBD polypeptide can bind complete preproteins, signal peptides, and mature regions.

Bulb Deletion Affects Binding of Mature Preprotein Regions—PBD is composed of a Bulb and a Stem (Fig. 1, *A* and *B*). Are both elements necessary for preprotein binding? Deletion of the β1 strand of the Stem prevents signal peptide binding to N68 (12). To determine whether the Bulb substructure of PBD is required for preprotein binding, we compared binding of preprotein segments with N68 and with N68ΔBulb. To this end, we developed a novel fluorescence-based assay.

Changes in the intrinsic fluorescence of N68 as a function of temperature were monitored upon the addition of either the nonfluorescent derivative CH5EEW49F or M13SP (Fig. 5*C*). In this assay, N68 displayed a characteristic $T_{m(app)}$ (44 °C) that was reduced when M13SP (by 5 °C) or CH5EEW49F (by 2.5 °C) were added, indicating that binding of either preprotein moiety to N68 caused its destabilization. The addition of either ligand had a similar effect on SecA (data not shown).

As observed with N68, the addition of M13SP caused a reduction in the $T_{m(app)}$ of N68ΔBulb (by 3.5 °C; Fig. 5*D*), suggesting that Bulb deletion does not prevent the N68/M13SP interaction. However, in contrast to what was observed for N68 (Fig. 5*C*), the addition of CH5EEW49F failed to cause any reduction in the $T_{m(app)}$ of N68ΔBulb (Fig. 5*D*), suggesting that Bulb deletion compromises binding of the mature region but not that of signal peptide to N68.

Our data suggested that binding of mature regions to SecA may require the Bulb (Fig. 5*D*), whereas binding of signal peptides to SecA may require the Stem (12).

Signal Peptide and Mature Preprotein Regions Induce Distinct PBD Conformations—We next sought to determine the effect of preprotein binding to PBD within the physiological context of the complete SecA and its fully functional N68 derivative. To this end, we examined the tryptic profile of SecA and N68 upon the addition of M13SP, CH5EE, or pCH5EE. In this experiment, the tryptic profile of SecA (data not shown) and N68 (Fig. 6*B*) are identical. Of all of the resulting peptides, only the five (indicated in Fig. 6*B*) that result from cleavage within or near PBD (Fig. 6*A*) were selected.

In the absence of preprotein fragments, three of the five peptides were seen (*lane 1*). When CH5EE was added, all five peptides were detected (*lane 2*). When M13SP was added none of the five peptides was detected (*lane 3*) due to significant protease protection of N68 (see remaining N68 amounts; *top*). This proteolytic protection presumably reflects a more compact conformational state. Trypsin activity is not inhibited by signal peptides (12). Finally, when pCH5EE was added three of the peptides were prominent, and the other two were barely detectable (*lane 4*).

It seemed that when complete preproteins, signal peptides, and mature regions bound to PBD attached to the DEAD motor, they stabilized distinct PBD conformations.

A 25-aa Mature Region Peptide Binds to PBD—We next sought to determine whether the full length of the mature preprotein region is required for binding to PBD. To address this possibility, a peptide that encompasses the first 25 mature region residues (hereafter referred to as CH5EE24–48; Fig. 4*A*) was chemically synthesized.

SecA (Fig. 7*A*, *lane 2*) and N68 (*lane 3*) bind to CH5EE24–48 immobilized on an optical biosensor, whereas a control protein did not (lane 1). Binding of CH5EE24–48 suppresses N68 ATPase (Fig. 7*B*) although clearly less efficiently than CH5EE, whereas a control peptide of similar length (p13) did not.

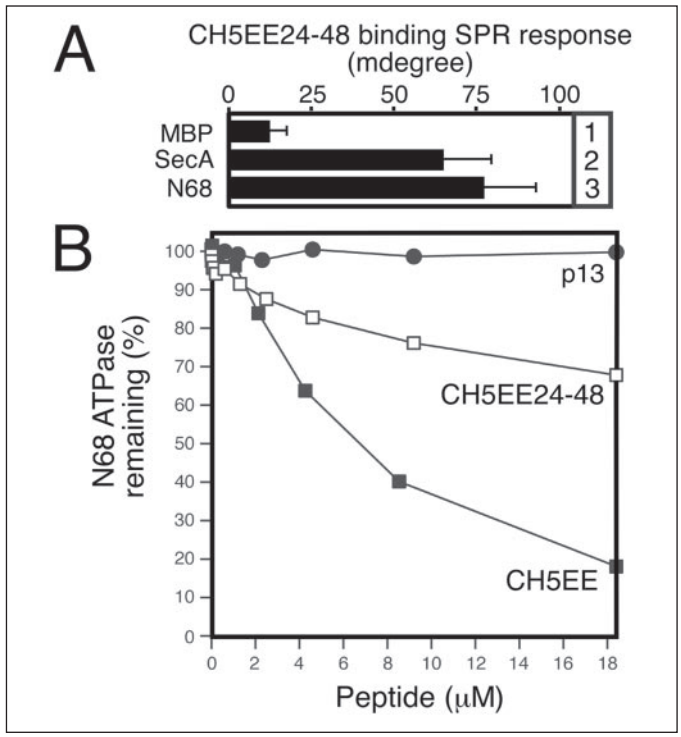

FIGURE 7. **CH5EE24–48 binding to PBD.** *A*, binding of proteins (1 μM; Buffer H) to CH5EE24–48 immobilized on a biosensor chip (as in Fig. 4*B*). Refractive index change was measured at equilibrium (t = 750 s). Maltose-binding protein (*MBP*) is used as a nonbinding control. *B*, suppression of N68 ATPase in the presence of the indicated peptides (as in Fig. 4*C*). p13 is a chemically synthesized peptide (25 aa) from the yeast α factor.

These data indicated that the N-terminal 25 aa of CH5EE can bind to PBD albeit inefficiently. This observation identified for the first time a minimal mature domain segment capable of binding to SecA.

DISCUSSION

Using two different preprotein substrates and derivative peptides, SecA mutants, and isolated domains, we determined that the second "substrate specificity" appendage of SecA (residues 221–377) is a PBD. Further biochemical dissection led to a two-subsite model: PBD binds signal peptides with its Stem and mature preprotein regions with its Bulb (Fig. 5). PBD is required for cell viability (Fig. 1*D*), protein translocation (Fig. 1*E*), preprotein-stimulated translocation ATPase (Fig. 3), and loading of preproteins to the membrane-embedded translocase (Fig. 2). PBD is therefore an essential element of the bacterial protein translocase catalytic cycle.

Signal peptide binding to the Stem of PBD is supported by several lines of evidence: (*a*) it is prevented by a deletion mutation in the Stem (12), (*b*) it can occur minimally within the aa 220–234 region of PBD that encompasses $Stem_{out}$ (12), (*c*) it does not require the Bulb (Fig. 5*D*), and (*d*) it prevents tryptic cleavage at Arg^{220} at the base of the Stem (Figs. 5*B* and 6*B*). Several hydrophobic residues on the Stem (see hypothetical model in Fig. 8) could provide a binding surface for residues of the signal peptide hydrophobic core shown by NMR studies to face the pocket (29). One of these residues suppresses defective signal peptides when mutated (A373V) (42). An extreme carboxyl-terminal SecA peptide may "shield" these hydrophobic residues in cytoplasmic SecA (10), thus preventing premature preprotein binding.

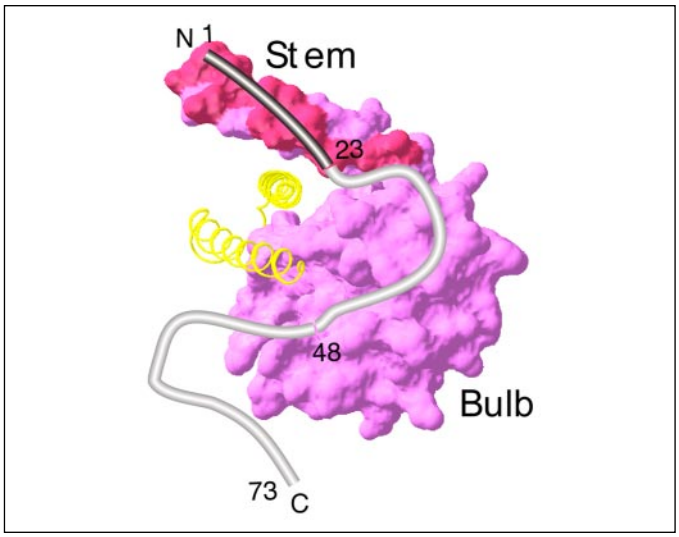

FIGURE 8. **Hypothetical model of the SecA PBD-preprotein interaction (see "Discussion" for details).** *B. subtilis* PBD (surface representation; hydrophobic side chains in *red*) is shown with bound pCH5EE (*gray tube*) and the associated IRA1 hairpin (*yellow ribbon*) (15). The assembly of pCH5EE on PBD is for visual demonstration only and has not been derived from high resolution structural analysis. Additional residues (not shown) from NBD and other parts of SecA may contribute to preprotein binding.

The mature preprotein region binds to SecA or N68 (Fig. 4*B* and TABLE FOUR) or to the isolated PBD (Fig. 5*B* and TABLE FOUR) but not to N68ΔBulb (Fig. 5*D*). Binding of the mature preprotein region invariably affects the accessibility of Bulb residue Lys^{360} (Figs. 5*B* and 6, *A* and *B*) in tryptic digestion assays. These data indicate that the Bulb binds mature preprotein regions. Such a specific binding function could explain why signalless preproteins still require SecA (43) and could rationalize previous cross-linking data (24). Cavities (10) and a groove formed between Stem, Bulb, NBD, and the IRA1 helical hairpin (Fig. 8) (16) could accommodate mature region peptides. Bulb mutations (44–47) may affect this binding.

Preproteins bind distinctly to the isolated PBD substructures identified here (Fig. 5*B* and TABLE FOUR). Nevertheless, the measured affinity of preproteins for PBD is reduced compared with that for the N1–419 fragment that contains both NBD and PBD (TABLE FOUR). We therefore anticipate that additional surfaces or particular residues from NBD may optimize preprotein binding. Electrostatic contacts between signal peptides and SecA were proposed to require NBD residues Asp^{217} and Glu^{218} at the root of the Stem (29). In other Superfamily 1 and 2 helicases, some DEAD motor residues are known to contribute to oligonucleotide substrate binding (48–50). In addition, the possibility cannot be excluded that preprotein molecules longer than the minimal preprotein used here may make additional contacts to other parts of SecA outside of PBD.

The small size of CH5EE24–48 suggests that a limited Bulb surface may be sufficient for a minimal primary binding. This site could reject positive charges in the mature region N terminus (51–54) and could act as a "molecular ruler" dictating the 20–30-aa step size seen in OmpA translocation (23, 55). Interestingly, a 30-residue region downstream of the signal peptide was proposed to act as an "export initiation domain" (54). However, binding of CH5EE24–48 is less efficient than that of CH5EE (Fig. 7*B*), suggesting that longer peptides may be better retained on the Bulb or may even engage additional parts of SecA.

Preprotein signal and mature region peptides can bind to their respective PBD subsites independently of each other in our *in vitro* assays (Fig. 5). Nevertheless, in *bona fide* secretory proteins signal peptides and mature regions are covalently adjoined and would therefore be expected to occupy both PBD subsites simultaneously. Preprotein binding to the two physically connected and spatially proximal subsites affects PBD conformation (Figs. 5*B* and 6*B*). This involves movement of residues at both the base of the Stem (Arg^{220}/Lys^{386}) and within the Bulb (Arg^{270}, Lys^{360}, and Lys^{329}) (Fig. 6*A*) and could influence Bulb swiveling around the Stem (16). The binding of signal peptide, mature region, and full-length preprotein affects PBD conformation in distinct ways (Figs. 5*B* and 6*B*). At the same time, the conformation of the Bulb is altered by signal peptide binding to the Stem (Fig. 5*B*) (12). These data raise the possibility that Stem-Bulb allosteric communication could facilitate "latching" of mature regions onto SecA. Tethering of PBD to NBD through a "rooted" Stem could optimize formation of this ternary complex by enhancing the measured affinity of isolated PBD for the preprotein (TABLE FOUR). NMR analysis indicated that once detached from NBD, the Stem region of PBD becomes unstructured (Fig. 5*A*). Binding to SecA promotes the acquisition of α-helical structure by signal peptides (29). This change in the signal peptide may affect the possible conformations that the Stem can acquire in SecA. The availability of NMR-based atomic resolution tools (Fig. 5*A*) (29) will greatly facilitate the analysis of PBD conformation and dynamics and its interaction with the preproteins in atomic detail.

Our data and those of others (10, 16, 17, 24, 25, 56) lead to a multistep working model where the mobile PBD domain acts as a flexible "control lever" that controls the mechanical activities of the SecY-bound SecA nanomotor. (*a*) Preprotein binds to PBD (Figs. 5*B* and 6*B* and TABLE FOUR) (24). (*b*) Preprotein binding modulates PBD conformation (Figs. 5*B* and 6) (12). (*c*) This change is transmitted through the Stem to the DEAD motor and affects the conformations of NBD (Fig. 6*B*), where PBD is physically rooted (Fig. 1, *A* and *B*), but also that of IRA2 as judged by tryptic accessibility of Arg^{586}/Lys^{609} (Fig. 6*B*; peptides p361–610 and p361–586). (*d*) Altered PBD conformation is also transmitted to the C-domain residues (10, 25), such as the helical hairpin of the IRA1 global regulator to which the Bulb is attached through defined contacts (Fig. 8, *yellow*) (15). (*e*) The net result of these conformational changes (Figs. 5*C* and 6*B*) detach the C-domain "staple" from its NBD and IRA2 binding sites (7, 14, 15), thereby loosening and destabilizing the DEAD motor (Figs. 5*C* and 6*B*). PBD mutations that display reduced ADP binding (TABLE ONE) and stabilization (TABLE TWO) may mimic this state. (*f*) "Loosening" of the DEAD motor affects ADP release (7, 17, 56) and nucleotide cycling (Fig. 4*C*). (*g*) ATP binding to the empty DEAD motor reverses the previous conformational events and drives the PBD-attached preprotein into the membrane. PBD could "rotate" between the two distinct conformational states identified crystallographically (10, 16). PBD may be free to acquire additional as yet unidentified conformational states when the C-domain is detached. (*h*) ATP hydrolysis, triggered via helicase Motif III (12, 21), partially releases the bound preprotein (23). (*i*) SecA returns to the stable ADP state (7, 17) and is primed for a new catalytic cycle triggered by preprotein binding to PBD.

Acknowledgments—We are grateful to D. Oliver and K. Ito for plasmids, K. Tokatlidis for comments, and Z. Tabaki, G. Trichas, and K. Daskalaki for preliminary experiments.

REFERENCES

1. Economou, A., and Wickner, W. (1994) *Cell* **78,** 835–843
2. Economou, A., Pogliano, J. A., Beckwith, J., Oliver, D. B., and Wickner, W. (1995) *Cell* **83,** 1171–1181
3. de Keyzer, J., van der Does, C., Kloosterman, T. G., and Driessen, A. J. (2003) *J. Biol. Chem.* **278,** 29581–29586
4. Koonin, E. V., and Gorbalenya, A. E. (1992) *FEBS Lett.* **298,** 6–8

5. Park, S. K., Kim, D. W., Choe, J., and Kim, H. (1997) *Biochem. Biophys. Res. Commun.* **235,** 593–597
6. Vrontou, E., and Economou, A. (2004) *Biochim. Biophys. Acta* **1694,** 67–80
7. Sianidis, G., Karamanou, S., Vrontou, E., Boulias, K., Repanas, K., Kyrpides, N., Politou, A. S., and Economou, A. (2001) *EMBO J.* **20,** 961–970
8. Caruthers, J. M., and McKay, D. B. (2002) *Curr. Opin. Struct. Biol.* **12,** 123–133
9. Sharma, V., Arockiasamy, A., Ronning, D. R., Savva, C. G., Holzenburg, A., Braunstein, M., Jacobs, W. R., Jr., and Sacchettini, J. C. (2003) *Proc. Natl. Acad. Sci. U. S. A.* **100,** 2243–2248
10. Hunt, J. F., Weinkauf, S., Henry, L., Fak, J. J., McNicholas, P., Oliver, D. B., and Deisenhofer, J. (2002) *Science* **297,** 2018–2026
11. Rocak, S., and Linder, P. (2004) *Nat. Rev. Mol. Cell Biol.* **5,** 232–241
12. Baud, C., Karamanou, S., Sianidis, G., Vrontou, E., Politou, A. S., and Economou, A. (2002) *J. Biol. Chem.* **277,** 13724–13731
13. Jarosik, G. P., and Oliver, D. B. (1991) *J. Bacteriol.* **173,** 860–868
14. Karamanou, S., Vrontou, E., Sianidis, G., Baud, C., Roos, T., Kuhn, A., Politou, A. S., and Economou, A. (1999) *Mol. Microbiol.* **34,** 1133–1145
15. Vrontou, E., Karamanou, S., Baud, C., Sianidis, G., and Economou, A. (2004) *J. Biol. Chem.* **279,** 22490–22497
16. Osborne, A. R., Clemons, W. M., Jr., and Rapoport, T. A. (2004) *Proc. Natl. Acad. Sci. U. S. A.* **101,** 10937–10942
17. Fak, J. J., Itkin, A., Ciobanu, D. D., Lin, E. C., Song, X. J., Chou, Y. T., Gierasch, L. M., and Hunt, J. F. (2004) *Biochemistry* **43,** 7307–7327
18. Hartl, F. U., Lecker, S., Schiebel, E., Hendrick, J. P., and Wickner, W. (1990) *Cell* **63,** 269–279
19. Lill, R., Dowhan, W., and Wickner, W. (1990) *Cell* **60,** 271–280
20. Randall, L. L., Crane, J. M., Liu, G., and Hardy, S. J. (2004) *Protein Sci.* **13,** 1124–1133
21. Papanikou, E., Karamanou, S., Baud, C., Sianidis, G., Frank, M., and Economou, A. (2004) *EMBO Rep.* **5,** 807–811
22. Fekkes, P., de Wit, J. G., van der Wolk, J. P., Kimsey, H. H., Kumamoto, C. A., and Driessen, A. J. (1998) *Mol. Microbiol.* **29,** 1179–1190
23. Schiebel, E., Driessen, A. J., Hartl, F. U., and Wickner, W. (1991) *Cell* **64,** 927–939
24. Kimura, E., Akita, M., Matsuyama, S., and Mizushima, S. (1991) *J. Biol. Chem.* **266,** 6600–6606
25. Ding, H., Mukerji, I., and Oliver, D. (2001) *Biochemistry* **40,** 1835–1843
26. Shinkai, A., Mei, L. H., Tokuda, H., and Mizushima, S. (1991) *J. Biol. Chem.* **266,** 5827–5833
27. Miller, A., Wang, L., and Kendall, D. A. (1998) *J. Biol. Chem.* **273,** 11409–11412
28. Triplett, T. L., Sgrignoli, A. R., Gao, F. B., Yang, Y. B., Tai, P. C., and Gierasch, L. M. (2001) *J. Biol. Chem.* **276,** 19648–19655
29. Chou, Y. T., and Gierasch, L. M. (2005) *J. Biol. Chem.* **280,** 32753–32760
30. Mitchell, C., and Oliver, D. (1993) *Mol. Microbiol.* **10,** 483–497
31. Roos, T., Kiefer, D., Hugenschmidt, S., Economou, A., and Kuhn, A. (2001) *J. Biol. Chem.* **276,** 37909–37915
32. Baud, C., Papanikou, E., Karamanou, S., Sianidis, G., Kuhn, A., and Economou, A. (2005) *Protein Expression Purif.* **40,** 336–339
33. Kiefer, D., and Kuhn, A. (1999) *EMBO J.* **18,** 6299–6306
34. Beck, K., Wu, L. F., Brunner, J., and Muller, M. (2000) *EMBO J.* **19,** 134–143
35. Millman, J. S., and Andrews, D. W. (1999) *J. Biol. Chem.* **274,** 33227–33234
36. Yoshihisa, T., and Ito, K. (1996) *J. Biol. Chem.* **271,** 9429–9436
37. Cavanagh, J., Fairbrother, W. J., Palmer, A. G., III, and Skelton, N. J. (1996) *Protein NMR Spectroscopy*, Academic Press, Inc., San Diego, CA
38. Brundage, L., Hendrick, J. P., Schiebel, E., Driessen, A. J., and Wickner, W. (1990) *Cell* **62,** 649–657
39. den Blaauwen, T., van der Wolk, J. P., van der Does, C., van Wely, K. H., and Driessen, A. J. (1999) *FEBS Lett.* **458,** 145–150
40. Chou, Y. T., Swain, J. F., and Gierasch, L. M. (2002) *J. Biol. Chem.* **277,** 50985–50990
41. Bassilana, M., Arkowitz, R. A., and Wickner, W. (1992) *J. Biol. Chem.* **267,** 25246–25250
42. Fikes, J. D., and Bassford, P. J., Jr. (1989) *J. Bacteriol.* **171,** 402–409
43. Derman, A. I., Puziss, J. W., Bassford, P. J., Jr., and Beckwith, J. (1993) *EMBO J.* **12,** 879–888
44. Kourtz, L., and Oliver, D. (2000) *Mol. Microbiol.* **37,** 1342–1356
45. Suzuki, H., Nishiyama, K., and Tokuda, H. (1998) *Mol. Microbiol.* **29,** 331–341
46. Khatib, K., and Belin, D. (2002) *Genetics* **162,** 1031–1043
47. Matsumoto, G., Nakatogawa, H., Mori, H., and Ito, K. (2000) *Genes Cells* **5,** 991–999
48. Velankar, S. S., Soultanas, P., Dillingham, M. S., Subramanya, H. S., and Wigley, D. B. (1999) *Cell* **97,** 75–84
49. Korolev, S., Hsieh, J., Gauss, G. H., Lohman, T. M., and Waksman, G. (1997) *Cell* **90,** 635–647
50. Kim, J. L., Morgenstern, K. A., Griffith, J. P., Dwyer, M. D., Thomson, J. A., Murcko, M. A., Lin, C., and Caron, P. R. (1998) *Structure* **6,** 89–100
51. Li, P., Beckwith, J., and Inouye, H. (1988) *Proc. Natl. Acad. Sci. U. S. A.* **85,** 7685–7689
52. Kajava, A. V., Zolov, S. N., Kalinin, A. E., and Nesmeyanova, M. A. (2000) *J. Bacteriol.* **182,** 2163–2169
53. Summers, R. G., and Knowles, J. R. (1989) *J. Biol. Chem.* **264,** 20074–20081
54. Andersson, H., and von Heijne, G. (1991) *Proc. Natl. Acad. Sci. U. S. A.* **88,** 9751–9754
55. Uchida, K., Mori, H., and Mizushima, S. (1995) *J. Biol. Chem.* **270,** 30862–30868
56. Schmidt, M., Ding, H., Ramamurthy, V., Mukerji, I., and Oliver, D. (2000) *J. Biol. Chem.* **275,** 15440–15448